

Temperature effect on multi-ionic species diffusion in saturated concrete

Nattapong Damrongwiriyanupap^{*1}, Linyuan Li^{2a}, Suchart Limkatanyu^{3b}
and Yunping Xi^{4c}

¹*Civil Engineering Program, School of Engineering, University of Phayao, Phayao 56000, Thailand*

²*Department of Mathematics and Statistics, University of New Hampshire,
Durham, NH 03824, United States*

³*Department of Civil Engineering, Faculty of Engineering, Prince of Songkla University,
Songkla 90112, Thailand*

⁴*Department of Civil, Environmental, and Architectural Engineering, University of Colorado at Boulder,
Boulder, CO 80309, United States*

(Received November 14, 2012, Revised August 7, 2013, Accepted September 16, 2013)

Abstract. This study presents the mathematical model for predicting chloride penetration into saturated concrete under non-isothermal condition. The model considers not only diffusion mechanism but also migration process of chloride ions and other chemical species in concrete pore solution such as sodium, potassium, and hydroxyl ions. The coupled multi-ionic transport in concrete is described by the Nernst-Planck equation associated with electro-neutrality condition. The coupling parameter taken into account the effect of temperature on ion diffusion obtained from available test data is proposed and explicitly incorporated in the governing equations. The coupled transport equations are solved using the finite element method. The numerical results are validated with available experimental data and the comparison shows a good agreement.

Keywords: chloride; concrete; temperature effect; Nernst-Planck equation; ionic diffusion

1. Introduction

Chloride-induced corrosion of reinforcing steel is one of the major problems in long-term durability of reinforced concrete structures. The problem occurs particularly in reinforced concrete structures subjected to chloride-rich environments such as marine structures in splash and tidal zones; bridge decks, and parking garages exposed to deicing salts. Chloride ions ingress into concrete through interconnected pore network in concrete. When chloride ions penetrate into

^{*}Corresponding author, Assistant Professor, E-mail: nattapong.da@up.ac.th

^aAssociate Professor, E-mail: linyuan@unh.edu

^bAssociate Professor, E-mail: suchart.l@psu.ac.th

^cProfessor, E-mail: yunping.xi@colorado.edu

concrete the chloride concentration of pore solution increases, and when the concentration reaches the critical value, the corrosion of reinforcement embedded in concrete starts. The corrosion of steel results in various deteriorations of reinforced concrete structures, such as cracking, spalling, and delamination of concrete cover due to the accumulation of the rust, and reduction of load carrying capacity of steel bars due to the reduced cross section area.

Many mathematical models have been developed to predict chloride ions transport in concrete structures. Under saturated condition, chloride penetration into concrete is mainly driven by concentration gradients of various diffusing ions in concrete (Zuo *et al.* 2010). Under non-saturated condition, chloride penetration into concrete is driven not only by the concentration gradients but also by moisture gradient, and many studies have shown that the moisture transport has a significant effect on the chloride diffusion in concrete (Ababneh *et al.* 2003, Abarr 2005, Suwito *et al.* 2005). Similarly, the moisture diffusion is influenced by the chloride penetration which accelerates the rate of moisture diffusion (Ababneh and Xi 2002). Under actual service condition, reinforced concrete structures are exposed to an environment with deicing salts, moisture variation, and temperature fluctuation. In this case, not only the moisture diffusion has an influence on the chloride transport, the temperature variation also has an effect on the chloride penetration. The temperature effect has been investigated by few researchers. Recently, Isteita (2009) conducted an experimental study on the temperature effect on chloride transport in concrete. It was found that the thermal effect contributed significantly to chloride penetration mechanism. With an increasing temperature, the rate of chloride penetration increased. A coupling parameter for the effect of temperature on the chloride transport was developed in the study. Over the years, there have been mathematical and numerical models developed to investigate chloride ions transport as well as multi-ionic transport in concrete, but there has been little research on the temperature effect. Yu and Page (1996), and Li and Page (1998, 2000) developed a mathematical model to simulate electrochemical chloride removal (ECR) from concrete and then Wang *et al.* (2005) applied the ECR model to perform the simulation of the mechanism of chloride ingress into concrete. Samson *et al.* (1999) conducted a theoretical study on ion diffusion mechanisms in cement-based materials. Later on, Samson and Marchand (1999) presented the mathematical model of ion diffusion mechanisms in porous media based on the Extended Nernst-Planck equation which accounts for electrostatic potential gradient. Recently, Marchand (2001) and Samson and Marchand (2007) developed a simulation model of multi-ionic transport in unsaturated cement-based materials exposed to aggressive chemical environments called STADIUM®. The mechanism of chloride penetration into non-saturated concrete was also investigated by Nguyen *et al.* (2006). The governing equations of the model were derived based on the Nernst-Planck and electro-neutrality equations. Then, the numerical results obtained from the model were compared with test data and a good agreement was observed.

As the actual condition of concrete structures exposed to various chloride environments is most likely non-isothermal rather than isothermal, the temperature variation has significant effect on the transport properties and chemical reaction of ions. In this study, we developed a mathematical model to predict the influence of temperature on chloride penetration into saturated concrete structures. The moisture diffusion was not considered in the model, while the effect of other ions in concrete pore solution was taken into account such as, Na⁺, K⁺, and OH⁻. And, the governing equation of temperature was described in terms of Fourier's law. Differing from those models proposed by Sætta *et al.* (1993) and Martin-Perez *et al.* (2000) in which temperature dependent transport parameters were used for the thermal effect, the present model took into account the coupled effect of temperature on chloride transport by an explicit term in the ionic flux equations.

There was a coupling parameter associated with the explicit term which was incorporated in the governing equations, and the value of coupling parameter and the model for the coupling parameter were obtained from Isteita study (2009). The governing equations were solved by the finite element method. The numerical results obtained from the present model were compared with available test data. The model can be applied to predict chloride penetration into saturated concrete structures under non-isothermal condition.

2. Basic formulation

The formulation of mathematical models for chloride transport can be done by two different approaches. One is based on Fick's first and second law which is related to the diffusion mechanism at macroscopic level (Sergi *et al.* 1992, Tang and Nilsson 1993, Saetta *et al.* 1993, Frey *et al.* 1994, Berke and Hicks 1994, Yu and Page 1996, Wee *et al.* 1997, Li and Page 1998, Xi and Bazant 1999, Ababneh *et al.* 2003, Suwito and Xi 2004, Zuo *et al.* 2012). This type of formulation is convenient for considering the single ion (the chloride ion) transport in concrete. The other formulation is based on the Nernst-Planck equation which takes into account the electro-chemical coupling phenomena. This type of formulation is necessary for characterizing the fully coupled multi-ionic transport in concrete. In the present study, the formulation of chloride ions and other chemical species in concrete pore solution, Na^+ , K^+ , and OH^- , is based on the Nernst-Planck equation. The governing equation of heat flow is described by the Fourier's law of heat conduction. The flux of each ionic species in a porous media without thermal effect can be expressed as

$$J_i = -D_i \nabla C_i - z_i D_i \left(\frac{F}{RT} \nabla \phi \right) C_i \quad (1)$$

where J_i is the flux of species i , D_i is the diffusion coefficient of species i , C_i is the concentration of species i in the solution, z_i is the charge number of species i , F is the Faraday constant, R is the gas constant, T is the temperature of material, and ϕ is the electrostatic potential. The mass balance equation for each ionic species can be written as

$$\frac{\partial C_i}{\partial t} = \frac{\partial (C_i + S_i)}{\partial t} = -\nabla J_i \quad (2)$$

By substituting Eq. (1) into Eq. (2), it gives

$$\frac{\partial C_i}{\partial t} = \frac{\partial (C_i + S_i)}{\partial t} = \frac{\partial C_i}{\partial C_i} \frac{\partial C_i}{\partial t} = \nabla \left(D_i \nabla C_i + z_i D_i \left(\frac{F}{RT} \nabla \phi \right) C_i \right) \quad (3)$$

in which C_i is the total chloride ion concentration which is the summation of free chloride ion (C_i) and bound chloride ion (S_i). When chloride ions penetrate into concrete, some of them can have chemical reaction with cement components and some of them can attach to the pore wall, and these chloride ions are called bound chlorides. The others are free to move through interconnected pores in concrete which are called free chlorides. $\partial C_i / \partial C_i$ is the chloride binding capacity. The binding capacity is applied only to chloride ion not to other species, Na^+ , K^+ , and OH^- (will be discussed in the section of material models), and thus there is no subscript i for C_i . The binding

capacity is related to the ratio of the free and bound chloride, and this parameter will be explained in the next section.

In order to solve the Nernst-Planck equation, another relation accounted for the electrostatic potential induced by ionic interaction is required. The electrostatic potential can be determined based on three different methods. Samson and Marchand (2007) solved the electrostatic potential for ion transport in cement-based materials by using Poisson's equation. As mentioned by Samson *et al.* (1999), the Poisson's equation can be used in more general cases. The nil current assumption was used by Li and Page (2000) and Wang *et al.* (2005). This method is based on the fact that there is no net current flow within the concrete pore solution due to the coupled ionic transport. The third method is based on electro-neutrality condition (i.e., the total charge of all ions in concrete is zero), which will be used in the present study. The electro-neutrality equation can be expressed as

$$\sum_{i=1}^n C_i z_i = 0 \quad (4)$$

in which C_i is the concentration of species i , z_i is the charge number of species i , and n is the number of ionic species. The main advantages of using electro-neutrality condition are the simplified governing equations, reduction of computational time, and less difficulty in computational schemes than the other two methods (Wang *et al.* 2005, Nguyen *et al.* 2006). The comparison among the nil current, Poisson's equation, and electro-neutrality condition used in modeling of chloride penetration into concrete was investigated by Nguyen *et al.* (2006) and Damrongwiriyanupap *et al.* (2011).

For the heat flow in concrete material, the heat flux can be simply expressed by Fourier's law of heat conduction equation

$$J_Q = -D_{T-T} \nabla T \quad (5)$$

in which J_Q is the heat flux, D_{T-T} is the thermal diffusivity of concrete, and T is temperature. The mass balance equation of heat flow is written as

$$\frac{\partial Q}{\partial t} = -\nabla J_Q \quad (6)$$

Combining Eqs. (5) and (6), the partial differential equation (PDE) governs the heat flow in concrete can be defined as

$$\frac{\partial Q}{\partial t} = \frac{\partial Q}{\partial T} \frac{\partial T}{\partial t} = \nabla(D_{T-T} \nabla T) \quad (7)$$

where $\partial Q / \partial T$ is the heat capacity of concrete.

In order to take into account the temperature effect on the transport of ions in concrete, the mass balance equations of each ionic species need to be reformulated. There are two ways to perform it. One is to use temperature dependent transport parameters in Eq. (3), and the other is to add an explicit term in Eq. (3) for the thermal effect. The latter method is used in the present study. The advantage is that the material models developed for the transport parameters in Eq. (3) under isothermal condition can be used, and the thermal effect is considered by the additional term. To this end, the original Nernst-Planck equation, Eq. (3), is modified as

$$\frac{\partial C_t}{\partial t} = \frac{\partial(C_i + S_i)}{\partial t} = \frac{\partial C_t}{\partial C_i} \frac{\partial C_i}{\partial t} = \nabla \left(D_i \nabla C_i + z_i D_i \left(\frac{F}{RT} \nabla \phi \right) C_i + D_{i-T} \nabla T \right) \quad (8)$$

in which D_{i-T} is the coupling parameter due to influence of temperature on the diffusions of ions. A model for this parameter will be described in the next section based on the experimental study of temperature effect on chloride penetration into saturated concrete by Isteita (2009). The effect of ionic diffusion on the heat conduction is considered as insignificant and thus not included in Eq. (7).

3. Material models

In order to solve the governing equations, Eqs. (7) and (8), and the electro-neutrality condition, Eq. (4), the material parameters involved in the equations must be determined first. These material parameters are ionic diffusion coefficients, ionic binding capacities, and the coupling parameters. In general, the material parameters depend on mix design and age of concrete and they are not constants. For instance, the chloride diffusion coefficient depends on water cement ratio, curing time, aggregate content and microstructure of cement paste, which in turn depends on concrete mix design parameters and age of concrete. In the present study the chloride diffusion coefficient is characterized by a material model proposed by Xi and Bazant (1999) which takes into account these influential parameters. Similarly, the chloride binding capacity can be described by the material model developed by Xi and Bazant (1999). A material model for the coupling parameter for the temperature effect will be developed based on available experimental results. For reader's convenience, the previously developed transport parameters will be introduced briefly, and then the model for the coupling parameter will be described in detail.

3.1 Chloride diffusion coefficient (D_{Cl})

The diffusion coefficient of chloride ions in concrete can be estimated using the multifactor method as follows

$$D_{Cl} = f_1(w/c, t_0) f_2(g_i) f_3(T) f_4(C_f) \quad (9)$$

in which $f_1(w/c, t_0)$ is a factor accounting for the influence of water-cement ratio (w/c) and curing time of concrete (t_0). The diffusion coefficient is higher when water-cement ratio increases. A formulation for $f_1(w/c, t_0)$ was proposed by Xi and Bazant (1999)

$$f_1(w/c, t_0) = \frac{28 - t_0}{62,500} + \left(\frac{1}{4} + \frac{(28 - t_0)}{300} \right) \left(\frac{w}{c} \right)^{6.55} \quad (10)$$

The second factor, $f_2(g_i)$, is incorporated for the effect of composite action of the aggregates and the cement paste on the diffusivity of concrete. This factor can be calculated by using the three phase composite model developed by Christensen (1979)

$$f_2(g_i) = D_{cp} \left(1 + \frac{g_i}{(1 - g_i)/3 + 1 / \left((D_{agg}/D_{cp}) - 1 \right)} \right) \quad (11)$$

where D_{agg} and D_{cp} are the chloride diffusivities of aggregates and cement paste, respectively. These two parameters can be determined by using the model proposed by Martys *et al.* (1994)

$$D = \frac{2(1 - (V_p - V_p^c))}{S^2} (V_p - V_p^c)^{4.2} \quad (12)$$

in which V_p is the porosity, S is the surface area, and V_p^c is the critical porosity (the porosity at which the pore space is first percolated). When Eq. (12) is used for the diffusivity of cement paste, D_{cp} , then V_p , S , and V_p^c are considered as the parameters for cement paste. The critical porosity may be taken as 3% for cement paste (Martys *et al.* 1994). Based on the study of Xi *et al.* (1994a), the surface areas of cement paste, S , can be estimated by the monolayer capacity, V_m , of adsorption isotherm of concrete which is proportional to S . The porosity, V_p , can be estimated by adsorption isotherm, at saturation ($H=1$). More detail on adsorption isotherm can be found in Xi *et al.* (1994a, b). The diffusivity of aggregates, D_{agg} , can be taken as a constant, and a proposed value is $1 \times 10^{-12} \text{ cm}^2/\text{s}$.

The third factor, $f_3(T)$, is to consider the effect of temperature on the diffusion coefficient of concrete. This can be calculated by using Arrhenius' law

$$f_3(T) = \exp \left[\frac{U}{R} \left(\frac{1}{T_0} - \frac{1}{T} \right) \right] \quad (13)$$

in which U is the activation energy of the diffusion process, R is the gas constant ($8.314 \text{ J mol}^{-1} \text{ K}^{-1}$), T and T_0 are the current and reference temperatures, respectively, in Kelvin ($T_0 = 296 \text{ K}$). According to the studies by Page *et al.* (1981) and Collepardi *et al.* (1972), the activation energy of the diffusion process depends on water-to-cement ratio, w/c , and cement type which can be found in Table 1.

The fourth factor, $f_4(C_f)$, describes the so-called concentration dependence, i.e. the dependence of the chloride diffusion coefficient on the free chloride concentration which can be expressed as follows

$$f_4(C_f) = 1 - k_{ion}(C_f)^m \quad (14)$$

where k_{ion} and m are two constants, 8.333 and 0.5, respectively. k_{ion} and m were obtained by Xi and Bazant (1999). It should be noted in Eq. (14) and all following equations that C_f is used to represent the free chloride concentration and C_i is for ionic concentration of all other ions.

Table 1 Activation energies for various cement paste

w/c	Ordinary portland cement (KJ/mol)	Cement with pozzolans (KJ/mol)
0.4	41.8 ± 4.0	-
0.5	41.8 ± 4.0	4.18
0.6	41.8 ± 4.0	-

3.2 Modelling of the material

As mentioned before, the ionic binding capacity is considered only for chloride ions. Other chemical species in concrete pore solution are assumed to be no binding capacity. The total chloride concentration, C_t , is the summation of free chloride, C_f , and bound chloride, C_b , which can be given by

$$C_t = C_f + C_b \quad (15)$$

The chloride binding capacity is defined as the incremental ratio of the free chloride content and total chloride content

$$\frac{dC_f}{dC_t} = \frac{1}{1 + \frac{dC_b}{dC_f}} \quad (16)$$

The term dC_b / dC_f can be obtained experimentally. By using the model developed by Xi and Bazant (1999), the chloride binding capacity can be expressed as

$$\frac{dC_f}{dC_t} = \frac{1}{1 + \frac{A10^B \beta_{C-S-H}}{35,450 \beta_{sol}} \left(\frac{C_f}{35.45 \beta_{sol}} \right)^{A-1}} \quad (17)$$

where A and B are two material constants related to chloride adsorption and equal to 0.3788 and 1.14, respectively (Tang and Nilsson 1993). The binding capacity depends on the two parameters, β_{sol} and β_{C-S-H} .

The parameter β_{sol} is described as the relationship between the volume of pore solution and weight of concrete (L/g)

$$\beta_{sol} = \frac{V_{sol}}{w_{conc}} = \frac{w_{sol}}{\rho_{sol} w_{conc}} = \frac{n(H,T)}{\rho_{sol}} \quad (18)$$

where V_{sol} is the volume of pore solution, w_{sol} is the weight of pore solution, w_{conc} is the weight of concrete, ρ_{sol} is the density of the pore solution (g/L) and is dependent on chloride concentration.

To simplify the calculation, the parameter ρ_{sol} can be estimated by using the density of pore water. The weight ratio of pore solution to concrete (w_{sol}/w_{conc}) represents chloride adsorption isotherm which is related to relative humidity, H , temperature, T , and pore structure of concrete. Due to a lack of test data on chloride isotherm, $n(H,T)$ may define as the isotherm of water adsorption instead of chloride isotherm. The adsorption isotherm of concrete can be described in terms of adsorption isotherm of cement paste and aggregate as follows

$$n(H,T) = f_{cp} n_{cp}(H,T) + f_{agg} n_{agg}(H,T) \quad (19)$$

in which f_{cp} and f_{agg} are the weight percentages of cement paste and aggregates, and $n_{cp}(H,T)$ and $n_{agg}(H,T)$ are the water adsorption isotherms of cement paste and aggregate, respectively.

The parameter β_{C-S-H} can be explained as the weight ratio of C-S-H gel to concrete (g/g). This factor is used to determine the effect of the cement composition and age of concrete on the volume fraction of C-S-H gel which is written as

$$\beta_{C-S-H} = \frac{w_{C-S-H}}{w_{total}} \quad (20)$$

where w_{C-S-H} and w_{total} are the weight of C-S-H gel and the total weight of concrete. The details of parameters $n(H,T)$ and β_{C-S-H} can be found in the paper by Xi (1994a).

The limitation of binding capacity based on the Freundlich isotherm, Eq. (17), is that the term $\partial C_f / \partial C_i = 0$ when the free chloride concentration, C_f , is zero because of $A < 1$. As a result, $\partial C_f / \partial C_i = 0$ leads to $\partial C_f / \partial t = 0$. This can be concluded that C_f is a constant at all time steps and equals to initial free chloride concentration. Thus, chloride diffusion never starts. To solve this problem, Tang and Nilsson (1993) suggested that the Freundlich isotherm can be used when C_f is large (> 0.01 mol/l), and the Langmuir isotherm is employed when C_f is small (< 0.05 mol/l). For these reasons, in the present study, the chloride binding capacity is represented by Langmuir isotherm for initial free chloride concentration ($C_f = 0$), and while the free chloride concentration is more than zero ($C_f > 0$), the chloride binding capacity can be determined by Eq. (17) based on Freundlich isotherm. The Langmuir isotherm is expressed as

$$\frac{1}{C'_b} = \frac{1}{k' C_{bm}} \frac{1}{C'_f} + \frac{1}{C_{bm}} \quad (21)$$

where k' is an adsorption constant, and C_{bm} is the bound chloride content at saturated monolayer adsorption (Tang and Nilsson 1993). C'_b and C'_f are the bound and free chloride contents used in Eq. (21). The units of these two parameters are in milligrams of bound chloride per gram of calcium silicate hydrate gel (mg/g) and in free chloride per liter of pore solution (mol/l), respectively, which is different from C_b and C_f . In the numerical simulation, it is necessary to use the consistent unit. Therefore, C'_b and C'_f can be converted and correlated to the unit of C_b and C_f as follows

$$C'_b = \frac{1,000 C_b}{\beta_{C-S-H}} \quad (22)$$

$$C_f' = \frac{C_f}{35.45\beta_{sol}} \quad (23)$$

Substituting Eqs. (22) and (23) into Eq. (21), yields

$$\frac{1}{C_b} = \frac{1,000}{\beta_{C-S-H}} \left[\frac{35.45\beta_{sol}}{k' C_{bm}} \frac{1}{C_f} + \frac{1}{C_{bm}} \right] \quad (24)$$

Eq. (24) can be re-expressed in a simple form as

$$C_b = \frac{1}{\beta + \frac{1}{\alpha C_f}} \quad (25)$$

in which

$$\alpha = \frac{k' C_{bm} \beta_{C-S-H}}{35,450 \beta_{sol}} \quad (26)$$

$$\beta = \frac{1,000}{\beta_{C-S-H} C_{bm}} \quad (27)$$

Derivative of Eq. (25) with respect to C_f yields

$$\frac{dC_b}{dC_f} = \frac{1}{\alpha (C_f)^2 \left(\beta + \frac{1}{\alpha C_f} \right)^2} \quad (28)$$

By substituting Eq. (28) into Eq. (16), the binding capacity based on Langmuir isotherm can be expressed as

$$\frac{dC_f}{dC_t} = \frac{1}{1 + \frac{dC_b}{dC_f}} = \frac{1}{1 + \frac{1}{\alpha \left(\beta C_f + \frac{1}{\alpha} \right)^2}} \quad (29)$$

Eq. (29) is used to calculate the binding capacity when free chloride concentration tends to zero, then the binding capacity is $1/(1 + \alpha)$. The parameter α can be calculated by using Eq. (26) and is dependent on many factors. As a result, α is definitely a non-zero number. The parameters in chloride binding capacity based on Langmuir isotherm can be obtained from Tang and Nilsson (1993) paper that is $1/C_{bm} = 0.1849$, $1/(k' C_{bm}) = 0.002438$, $k' = 75.841$, and $C_{bm} = 5.4083$.

3.3 Coupling parameter (D_{i-T})

The coupling parameter presented in this study was proposed by Isteita (2009). The parameter was evaluated based on the experimental study of temperature effect on chloride penetration into saturated concrete. The results from the experiment showed that the effect of temperature on chloride diffusion is very significant and the coupled effect of temperature on chloride diffusion in concrete should be taken into account. The influence of temperature on ions diffusion is related to Soret effect, which is the occurrence of a diffusion flux due to the temperature gradient. Then, the coupling parameter was derived by using a multifactor approach. It was also found that the coupling parameter was not constant but depended on chloride concentration, age of concrete, and temperature. This can be obtained by curve fitting of the test data written as

$$D_{Cl-T} = 5 \times 10^{-8} C_f f_1(t) f_2(T) \quad (30)$$

Based on the Soret effect, the heat flow in concrete can carry not only chloride ions but also other ions in concrete pore solution so that we may apply this coupling parameter to all ionic species (Cl^- , Na^+ , K^+ , and OH^-), it gives,

$$D_{i-T} = D_{Cl-T} = 5 \times 10^{-8} C_f f_1(t) f_2(T) \quad (31)$$

in which D_{i-T} is the coupling parameter due to temperature effect on each ionic species i ; C_f is the free chloride concentration; the first factor, $f_1(t)$, is the factor accounting for the age effect of concrete which is relevant to hydration reactions of cement paste given by Eq. (32)

$$f_1(t) = 4t^{-1} \quad (32)$$

where t is the age of concrete. The second factor, $f_2(T)$, takes into account the influence of temperature which is described by the definition of Arrhenius's law

$$f_2(T) = \text{Exp}\left(0.1 \frac{U}{R} \left(\frac{1}{T_{ref}} - \frac{1}{T}\right)\right) \quad (33)$$

where U is the activation energy of the diffusion process; R is the gas constant; and T and T_{ref} are current and reference temperature, respectively.

4. Numerical simulation

Numerical simulations are performed to study the effect of temperature on transport of chloride and others ionic species in saturated concrete and to compare with the available test data. The material models discussed in the previous sections are incorporated in the governing equations, Eqs. (4), (7) and (8). In the present study, the finite element method is employed for solving partial differential equations of ionic transport and the heat conduction in saturated concrete. The numerical study was focused on NaCl penetrating into concrete sample from the top surface of a concrete slab. The ions in concrete pore solution, Na^+ , K^+ , and OH^- , are considered in the numerical analysis. The material parameters and input data for numerical simulations related to the governing equations are shown in Table 2. This information include diffusion coefficients, initial concentration at the top surface, and initial concentration in concrete pore solution of each ionic

species, water-to-cement ratio, and volume fraction of aggregate. The concentration of alkali ions in pore solution, Na^+ and K^+ , are obtained from the cement manufacturing company which provided the chemical composition of cement used in the experimental study. The concentration of hydroxyl ion can be calculated by using electro-neutrality condition. The numerical simulations were performed under saturated condition. This means that the relative humidity inside and outside concrete sample are equal to 100%. As a result, there is no effect from moisture gradient on multi-ions diffusion in the present study. The units of all ionic concentrations are in mol/l except for the total chloride which is in grams of chloride/gram of concrete weight (g/g) as mentioned in AASHTO T 259 and AASHTO T 260.

Table 2 Material parameters and input data

	Cl	Na	K	OH
Diffusion coefficient (m^2/s)	D_{Cl} (Eq. 9)	2.7×10^{-11}	3.9×10^{-11}	5.28×10^{-10}
Initial pore solution concentration (mol/l)	0.0	0.0389	0.0995	0.1384
Heat capacity ($\text{J/kg } ^\circ\text{C}$)		$\S 1,000$		
Thermal diffusivity ($\text{W/m } ^\circ\text{C}$)		$\S 2$		
Chloride binding capacity		dC_f / dC_t (Eqs. 17 and 29)		
Coupling parameter		D_{i-T} (Eq. 31)		
Water-cement ratio		0.55		
Volume fraction of aggregate		0.65		
Cement type		I/II		

* The values are taken from Wang *et al.* (2005).

§ The values are taken from Isgor and Razaqpur (2004).

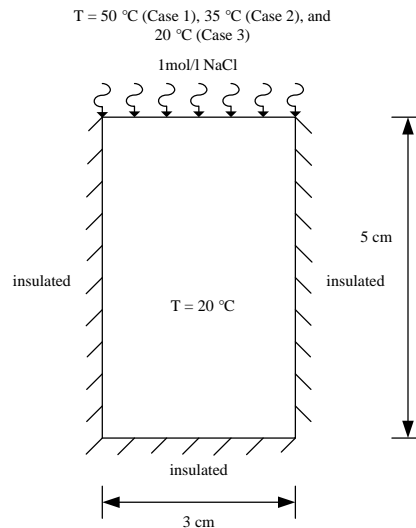


Fig. 1 Geometry and boundary conditions of concrete specimen used for numerical analysis

The geometry of concrete sample used in numerical simulation is shown in Fig. 1. It is a 3 cm by 5 cm concrete specimen. The concrete sample is exposed to 1 mol/l NaCl solution on the top surface. The other boundaries are assumed to be insulated. The moisture condition inside the concrete sample is assumed to be fully saturated, 100% RH. The concrete sample is divided into 400 elements and 451 nodes by using isoparametric elements for the finite element analysis. In order to compare with available test data, the numerical simulations were conducted in three different cases as shown in Fig. 1. For case 1, 2, and 3, the temperatures on the top surface of concrete samples are 50°C, 35°C, and 20°C, respectively. And, the initial temperature inside specimens is specified as 20°C. This means that there is no temperature gradient for case 3.

5. Numerical results and discussion

The concentration profiles of chloride, sodium, potassium, and hydroxyl ions exposed to 1 mol/l NaCl solution at different initial temperature conditions ($T = 50^\circ\text{C}$, 35°C , and 20°C) are shown in Figs. 2, through 13. At $T = 50^\circ\text{C}$, as shown in Figs. 2 through 5, the concentration of chloride is remarkably influenced by temperature, especially at the depth close to the exposed surface which can be seen as an instant increase from Fig. 2. After this point, the concentration decreases with increasing depth. Fig. 3 shows the concentration profile of sodium which decreases when the depth of penetration increases. It is evident from Figs. 2 and 3 that the concentration gradients of sodium and chloride share the same trend from the top to bottom surface. This is because the initial concentration of these two ions inside the specimen is lower than that at the exposed surface.

For hydroxyl ions, the concentration increases when the depth of penetration increases, as shown in Fig. 4, which is due to the fact that the hydroxyl ions have a lower concentration at the exposed surface than the deep part of the concrete slab. In fact, there are no hydroxyl ions at the top (exposed) surface. The concentration gradient of hydroxyl is in the reverse direction of chloride and sodium ions. The distribution profile of potassium starts from zero at the exposed surface, similar to hydroxyl ions, and increases until reaching the peak, as shown in Fig. 5, which is the point adjacent to the exposed surface and then drops to the initial value of pore solution concentration. The main reason for this reversal (increase and then decrease) is due to the electro-neutrality condition in which the negatively charged ions, Cl^- and OH^- , must be balanced by the positively charged ions such as K^+ .

At $T = 35^\circ\text{C}$ the coupled temperature effect has less impact than at $T = 50^\circ\text{C}$ because of the lower temperature gradient. As noticed from Figs. 6 and 7, there is no instant increase of chloride and sodium profiles at the depth close to exposed surface. Thus, at $T = 35^\circ\text{C}$, chloride and sodium concentrations decrease monotonically, while Figs 8 and 9 show that hydroxyl and potassium concentrations increase with increasing depth from exposed surface. Figs. 10 through 13 illustrate the distribution profiles of chloride, sodium, hydroxyl, and potassium ions at $T = 20^\circ\text{C}$. It can be seen that the concentration profiles of these four ionic species have the same trends as obtained from $T = 35^\circ\text{C}$. The transport mechanisms of the four ions at $T = 20^\circ\text{C}$ are mainly due to diffusion and migration processes because of no temperature gradient. The relationship between concentration and exposure time of these four ionic species can be observed from Figs. 2 through 13 that, at any fixed depth, the concentrations of chloride and sodium ions are higher with the longer period of exposure whereas the concentrations of potassium and hydroxyl ions tend to decrease with an increase of exposure time.

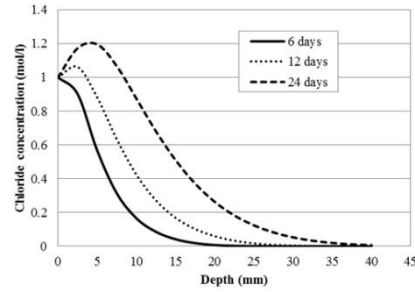


Fig. 2 Chloride concentration profiles at $T = 50^{\circ}\text{C}$

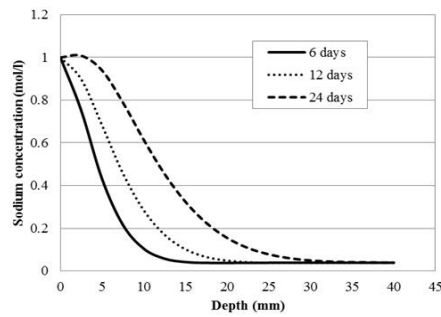


Fig. 3 Sodium concentration profiles at $T = 50^{\circ}\text{C}$

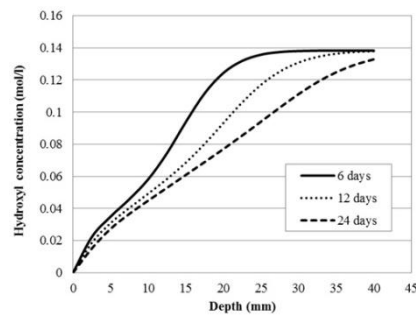


Fig. 4 Hydroxyl concentration profiles at $T = 50^{\circ}\text{C}$

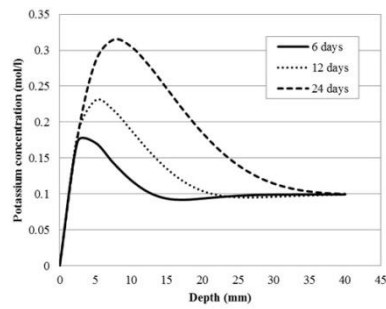
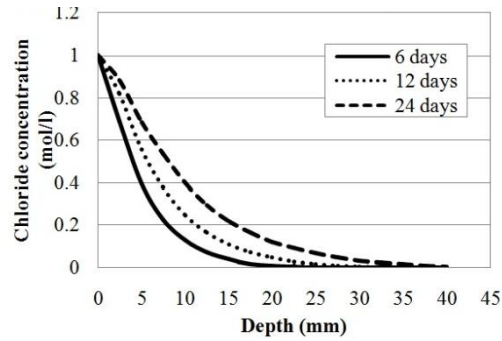
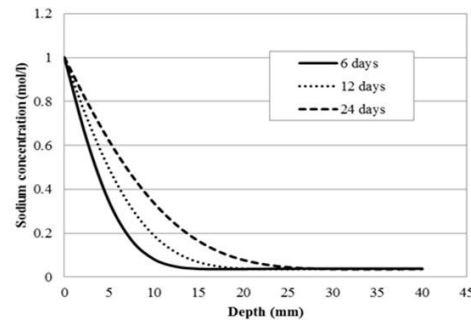
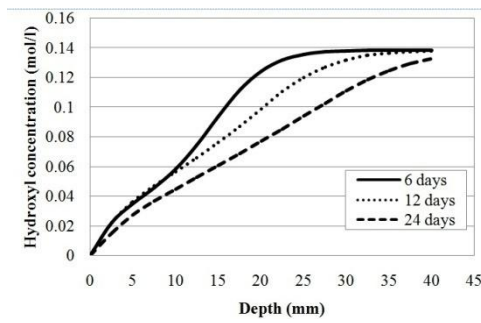
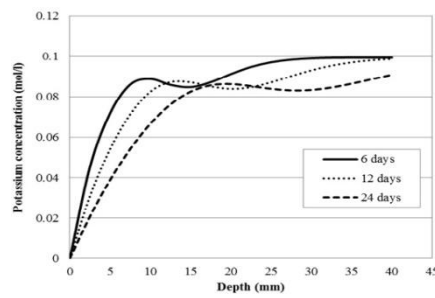


Fig. 5 Potassium concentration profiles at $T = 50^{\circ}\text{C}$

Fig. 6 Chloride concentration profiles at $T = 35^{\circ}\text{C}$ Fig. 7 Sodium concentration profiles at $T = 35^{\circ}\text{C}$ Fig. 8 Hydroxyl concentration profiles at $T = 35^{\circ}\text{C}$ Fig. 9 Potassium concentration profiles at $T = 35^{\circ}\text{C}$

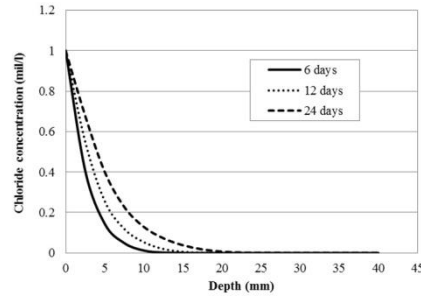


Fig. 10 Chloride concentration profiles at $T = 20^{\circ}\text{C}$

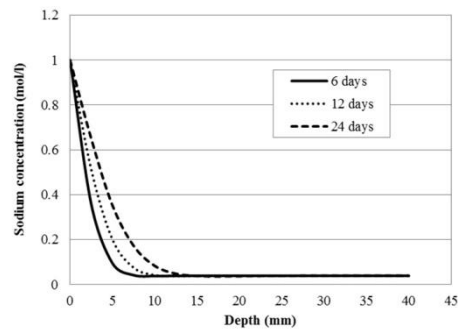


Fig. 11 Sodium concentration profiles at $T = 20^{\circ}\text{C}$

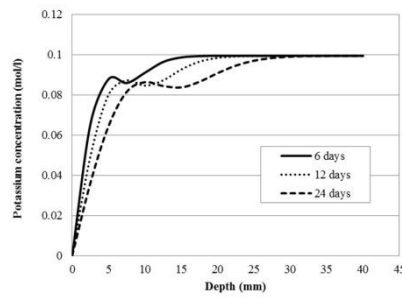


Fig. 12 Hydroxyl concentration profiles at $T = 20^{\circ}\text{C}$

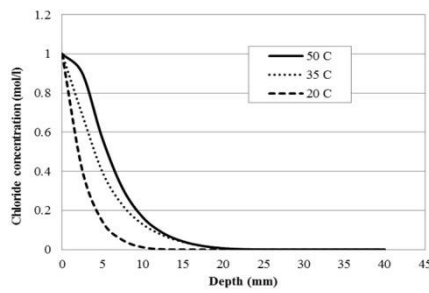


Fig. 13 Potassium concentration profiles at $T = 20^{\circ}\text{C}$

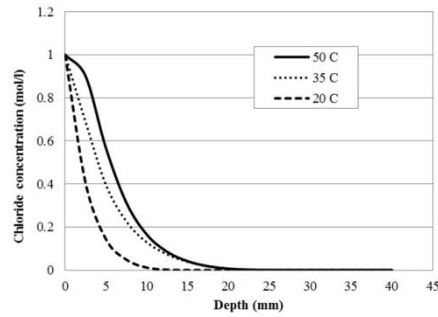


Fig. 14 Chloride concentration profiles exposed to 1 mol/l NaCl solution at 6days

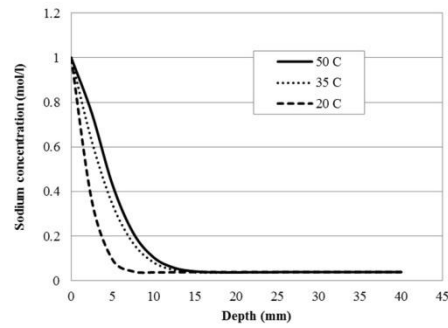


Fig. 15 Sodium concentration profiles exposed to 1 mol/l NaCl solution at 6days

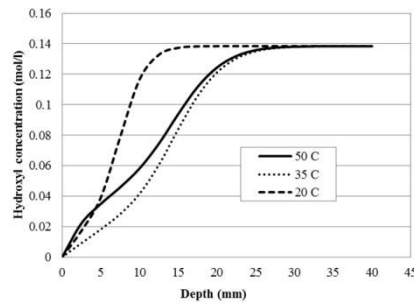


Fig. 16 Hydroxyl concentration profiles exposed to 1 mol/l NaCl solution at 6days

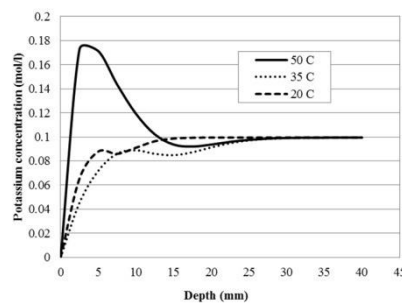


Fig. 17 Potassium concentration profiles exposed to 1 mol/l NaCl solution at 6days

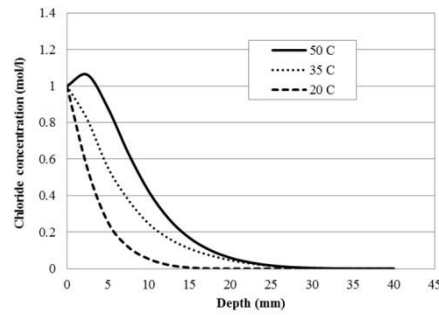


Fig. 18 Chloride concentration profiles exposed to 1 mol/l NaCl solution at 12days

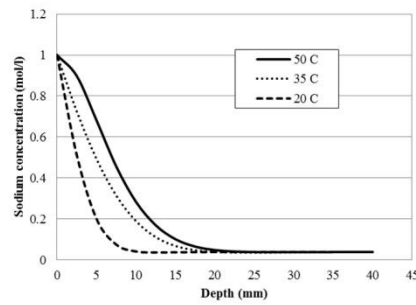


Fig. 19 Sodium concentration profiles exposed to 1 mol/l NaCl solution at 12days

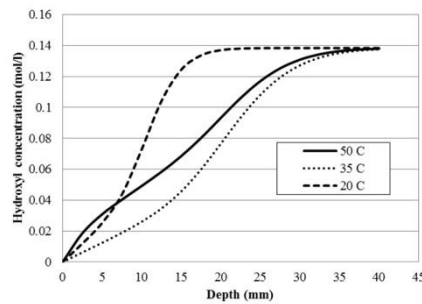


Fig. 20 Hydroxyl concentration profiles exposed to 1 mol/l NaCl solution at 12days

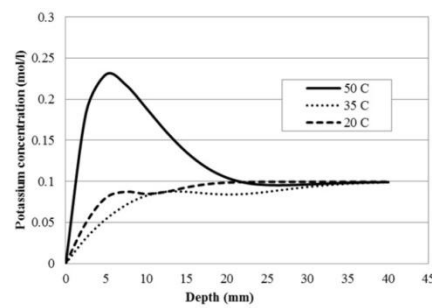


Fig. 21 Potassium concentration profiles exposed to 1 mol/l NaCl solution at 12days

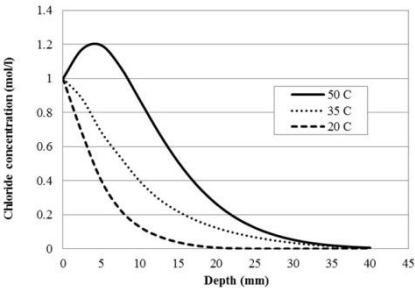


Fig. 22 Chloride concentration profiles exposed to 1 mol/l NaCl solution at 24days

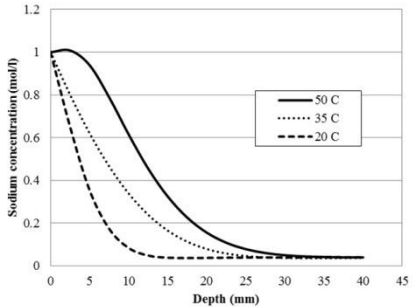


Fig. 23 Sodium concentration profiles exposed to 1 mol/l NaCl solution at 24days

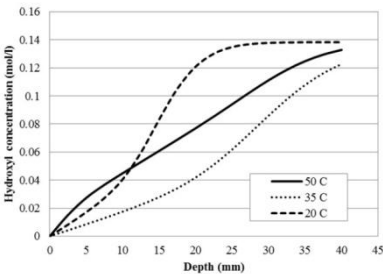


Fig. 24 Hydroxyl concentration profiles exposed to 1 mol/l NaCl solution at 24days

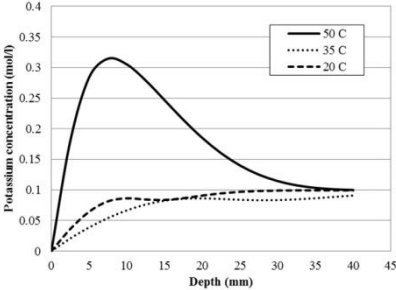


Fig. 25 Potassium concentration profiles exposed to 1 mol/l NaCl solution at 24days

Figs. 14 through 25 show the influence of temperature on ionic diffusion at different times of exposure (6, 12, and 24 days of exposure). One can see from these plots that the variations of concentration profiles of the four ionic species can be observed with increasing temperature. The higher the temperature gradient, the more significant of the coupled temperature effect. At 6, 12, and 24 days of exposure, with increasing temperature, the concentration of chloride and sodium ions increase, at any fixed depth, which is accelerated by temperature gradient. Moreover, at $T = 50^\circ\text{C}$, at any times of exposure, chloride and sodium ions are accelerated by higher temperature gradient when compared with $T = 35^\circ\text{C}$. Therefore, At $T = 50^\circ\text{C}$, hydroxyl ion diffuses faster to satisfy the electro-neutrality condition with positively charged ions, Na^+ and K^+ . From Figs. 16 and 24, hydroxyl concentration at $T = 50^\circ\text{C}$ is slightly higher than at $T = 20^\circ\text{C}$ at the depth close to the exposed surface due to the electro-neutrality condition. With increasing depth from this area, hydroxyl concentration at $T = 20^\circ\text{C}$ is higher than both at $T = 50^\circ\text{C}$ and 35°C because the diffusion rate of hydroxyl ion is slowed down by temperature gradient. For potassium ions, when temperature increases from 20°C to 35°C the concentration at higher temperature is lower than at the lower temperature, at any times of exposure. This is mainly due to the heat flux which is in the reverse direction of concentration gradient of potassium so that the diffusion rate of potassium is actually reduced by the temperature gradient. However, when temperature reaches $T = 50^\circ\text{C}$ the concentration is higher than at $T = 35^\circ\text{C}$ and 20°C . This is because at this temperature range, the transport mechanism of potassium is dominated by the electro-neutrality condition. As noticed from numerical results, we can conclude that the concentrations of four ionic species are significantly influenced by temperature variation.

6. Comparison with test data

The results of total chloride concentration (in gram of chloride per gram of concrete) predicted by the present model are plotted and compared with the available test data obtained from Isteita (2009). The chloride ponding tests were conducted at different initial temperature conditions at the exposed (top) surface. The comparisons between numerical and experimental results exposed to 3% NaCl at $T = 50^\circ\text{C}$ for 6 and 12 days of exposure are shown in Figs. 26 and 27, respectively. Figs. 28 and 29 present the comparisons at $T = 35^\circ\text{C}$ for specimens exposed to 3% NaCl for 6 and

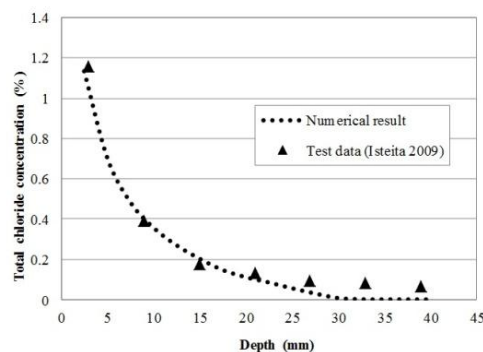


Fig. 26 The comparison between numerical result and test data at 6 days of specimens exposed to $T = 50^\circ\text{C}$

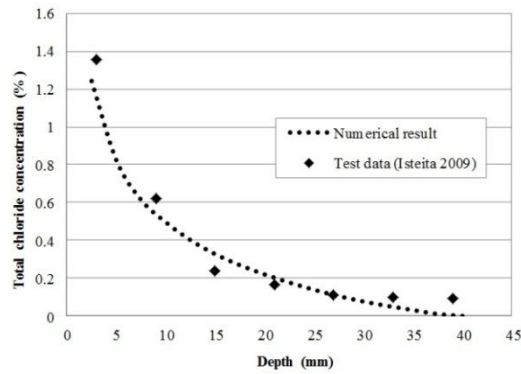


Fig. 27 The comparison between numerical result and test data at 12 days of specimens exposed to $T = 50^{\circ}\text{C}$

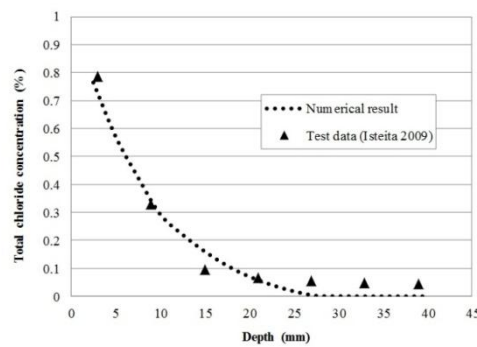


Fig. 28 The comparison between numerical result and test data at 6 days of specimens exposed to $T = 35^{\circ}\text{C}$

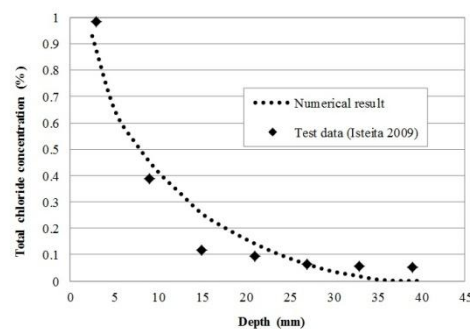


Fig. 29 The comparison between numerical result and test data at 12 days of specimens exposed to $T = 35^{\circ}\text{C}$

12 days of exposure, respectively. It can be seen from Figs 26 through 29, at $T = 50^{\circ}\text{C}$ and $T = 35^{\circ}\text{C}$, that the results obtained from the present model have a good agreement with test data. Therefore, the present comprehensive model taking into account the diffusion mechanisms, ionic

interaction, and the coupled temperature effect can be used to predict the chloride penetration into concrete structures not only in isothermal condition but also in non-isothermal condition.

7. Conclusions

1. A mathematical model is developed for predicting the chloride penetration into saturated concrete structures under non-isothermal condition. The model takes into account diffusion mechanism due to ionic concentration gradient and migration processes due to ionic interaction of chloride ions and other chemical species in concrete pore solution (Na^+ , K^+ , and OH^-) which is described by the Nernst-Planck equation.

2. The heat flow in concrete is considered in this study which is described by Fourier's heat conduction equation. A coupling term obtained from available test data is proposed. Then, the ionic flux equations are modified by incorporating explicitly the coupling term for the temperature effect. The numerical simulations are performed by assuming a concrete sample exposed to chloride solution (NaCl) at different initial temperature conditions. The governing equations are solved by using the finite element method.

3. Material models for the transport parameters are included in the numerical simulation. The diffusion coefficients and the chloride binding capacity are obtained from literature, and the coupling parameters for the temperature effect are developed based on available test data.

4. The numerical results show that the coupling term contributes significantly to the diffusion mechanism of four ionic species (Cl^- , Na^+ , K^+ , and OH^-) by accelerating the penetration rate of chloride and sodium concentration. However, potassium and hydroxyl concentration profiles vary by the temperature effect and electro-neutrality condition.

5. The numerical results predicted by the present model are validated with the available test data. The comparison shows that the total chloride profiles obtained from the model have a good agreement with the test data.

6. The present comprehensive model can be used to predict the chloride ingress into saturated concrete structures under both isothermal and non-isothermal conditions.

Acknowledgements

The financial supports from the Thailand Research Fund (TRF) under Grant MRG5580222 and under NSF grant CMMI-0727749 to the University of Colorado Boulder and the University of New Hampshire are gratefully acknowledged.

References

- Ababneh, A. and Xi, Y. (2002), "An experimental study on the effect of chloride penetration on moisture diffusion in concrete", *Mater. Struct.*, **35**, 659-664.
- Ababneh, A., Benboudjema, F. and Xi, Y. (2003), "Chloride penetration in nonsaturated concrete", *J. Mater. Civ. Eng., ASCE*, **15**(2), 183-191.
- Abarr, L. (2005), "The effect of moisture diffusion on chloride penetration", M.S. Thesis, the University of Colorado at Boulder.
- Berke, N.S. and Hicks, M.C. (1994), "Predicting chloride profiles in concrete", *Corros.*, March, 234-239.
- Christensen, R.M. (1979), "Mechanics of composite materials", Wiley Interscience, New York.

- Colleparidi, M., Marciall, A. and Turriziani, R. (1972), "Penetration of chloride ions in cement pastes and concrete", *J. American Ceram. Soc.*, **55**(10), 534-535.
- Damrongwiriyanupap, N., Li L.Y. and Xi, Y. (2011), "Coupled diffusion of chloride and other ions in saturated concrete", *Front. Archit. Civ. Eng. China*, **5**(3), 267-277.
- Frey, R., Balogh, T. and Balazs, G.L. (1994), "Kinetic method to analyze chloride diffusion in various concretes", *Cement. Concrete Res.*, **24**(5), 863-873.
- Isgor, B. and Razacpur, G. (2004), "Finite element modeling of coupled heat transfer, moisture transport and carbonation processes in concrete structures", *Cement. Concrete Res.*, **1**, 57-73.
- Isteita M. (2009), "The effect of thermal conduction on chloride penetration in concrete", M.S. Thesis, the University of Colorado at Boulder.
- Li, L.Y. and Page, C.L. (1998), "Modeling of electrochemical chloride extraction from concrete: influence of ionic activity coefficients", *Comput. Mater. Sci.*, **9**, 303-308.
- Li, L.Y. and Page, C.L. (2000), "Finite element modeling of chloride removal from concrete by an electrochemical method", *Corros. Sci.*, **42**, 2145-2165.
- Marchand, J. (2001), "Modeling the behavior of unsaturated cement systems exposed to aggressive chemical environments", *Mater. Struct.*, **34**, 195-200.
- Martin-Perez, B., Zibara, H., Hooton, R.D. and Thomas, M.D.A. (2000), "A study of the effect of chloride binding on service life predictions", *Cement. Concrete Res.*, **30**, 1215-1223.
- Martys, N.S., Torquato, S. and Bentz, D.P. (1994), "Universal scaling of fluid permeability for sphere packings", *Phys. Rev., E*, **50**(1), 403-408.
- Nguyen, T.Q., Baroghel-Bouny, V. and Dangla, P. (2006), "Prediction of chloride ingress into saturated concrete on the basis of multi-species model by numerical calculations", *Comput. Concr.*, **3**(6), 401-422.
- Page, C.L., Short, N.R. and El Tarras, A. (1981), "Diffusion of chloride ions in hardened cement paste", *Cement. Concrete Res.*, **11**(3), 395-406.
- Saetta, A.V., Scotta, R.V. and Vitaliani, R.V. (1993), "Analysis of chloride diffusion into partially saturated concrete", *ACI Mater. J.*, **90**(5), 441-451.
- Samson, E. and Marchand, J. (1999), "Numerical solution of the extended nernst-planck model", *J. Colloid. Interface. Sci.*, **215**, 1-8.
- Samson, E. and Marchand, J. (2007), "Modeling the transport of ions in unsaturated cement-based materials", *Comput. Struct.*, **85**, 1740-1756.
- Samson, E., Marchand, J., Robert, J.L. and Bournazel, J.P. (1999), "Modelling ion diffusion mechanisms in porous media", *Int. J. Numer. Meth. Eng.*, **46**, 2043-2060.
- Sergi, G., Yu, S.W. and Page, C.L. (1992), "Diffusion of chloride and hydroxyl ions in cementitious materials exposed to a saline environment", *Mag. Concr. Res.*, **44**, 63-72.
- Suwito, A. and Xi, Y. (2004), "Service life of reinforced concrete structures with corrosion damage due to chloride attack", In: *Frangopol, D.M., Bruhwiler, E., Faber, M.H. and Adey, B. (eds), Life-Cycle Performance of Deteriorating Structures: Assessment, Design and Management*, Special Publication of ASCE, 207-218.
- Suwito, Cai X.C. and Xi Y. (2006), "Parallel finite element method for coupled chloride penetration and moisture diffusion in concrete", *Int. J. Num. Anal. Mod.*, **3**(4), 481-503.
- Tang, L. and Nilsson, L.O. (1993), "Chloride binding capacity and binding isotherms of OPC pastes and mortars", *Cement Concrete Res.*, **23**, 247-253.
- Wang, Y., Li, L.Y. and Page, C.L. (2005), "Modeling of chloride ingress into concrete from a saline environment", *Build. Environ.*, **40**, 1573-1582.
- Wee, T.H., Wong, S.F., Swadiwudhipong, S. and Lee, S.L. (1997), "A prediction method for long-term chloride concentration profiles in hardened cement matrix materials", *ACI Mater. J.*, **94**(6), 565-576.
- Xi, Y. and Bazant, Z. (1999), "Modeling chloride penetration in saturated concrete", *J. Mater. Civil Eng., ASCE*, **11**(1), 58-65.
- Xi, Y., Bazant, Z.P. and Jennings, H.M. (1994a), "Moisture diffusion in cementitious materials: adsorption isotherm", *J. Adv. Cement-Based Mater.*, **1**, 248-257.
- Xi, Y., Bazant, Z.P., and Jennings, H.M. (1994b), "Moisture diffusion in cementitious materials: moisture

- capacity and diffusivity”, *J. Adv. Cement-Based Mater.*, **1**, 258-266.
- Yu, S.W. and Page, C.L. (1996), “Computer simulation of ionic migration during electrochemical chloride extraction from hardened concrete”, *Brit. Corros. J.*, **31**, 73-75.
- Zuo, X.B., Sun, W., Yu, C. and Wan, X.R. (2010), “Modeling of ion diffusion coefficient in saturated concrete”, *Comput. Concr.*, **7**(5), 421-434.
- Zuo, X.B., Sun, W., Li, H. and Zhao, Y.K. (2012), “Modeling of diffusion-reaction behavior of sulfate ion in concrete under sulfate environments”, *Comput. Concr.*, **10**(1), 79-93.

CC